

Biodegradable polycaprolactone scaffold with controlled porosity obtained by modified particle-leaching technique

M. Lebourg · R. Sabater Serra · J. Más Estellés ·
F. Hernández Sánchez · J. L. Gómez Ribelles ·
J. Suay Antón

Received: 10 January 2006 / Accepted: 18 September 2007 / Published online: 30 October 2007
© Springer Science+Business Media, LLC 2007

Abstract Scaffold with controlled porosity constitute a cornerstone in tissue engineering, as a physical support for cell adhesion and growth. In this work, scaffolds of polycaprolactone were synthesized by a modified particle leaching method in order to control porosity and pore interconnectivity; the aim is to observe their influence on the mechanical properties and, in the future, on cell adhesion and proliferation rates. Low molecular weight PEMA beads with an average size of 200 μm were sintered with various compression rates in order to obtain the templates (negatives of the scaffolds). Then the melt polycaprolactone was injected into the porous template under nitrogen pressure in a custom made device. After cooling and solidifying of the melt polymer, the porogen was removed by selective dissolution in ethanol. The porosity and morphology of the scaffold were studied as well as the mechanical properties. Porosities from 60% to 85% were reached; it was found that pore interconnectivity logically increases with increasing porosity, and that mechanical strength decreases with increasing porosity. Because of their interesting properties and interconnected structure, these scaffolds are expected to find useful applications as a cartilage or bone repair material.

1 Introduction

Cartilage repair is very difficult because of its poor cell density and lack of vascularization [1–3]. New developments in biomedical science point on tissue engineering strategies to obtain the desired regeneration. Tissue engineering combines the use of cells, scaffolds and signalling substances to regenerate a tissue both physically and biologically. Scaffolds are porous structures that play the role of a synthetic extracellular matrix, and permit cell adhesion, proliferation and differentiation [4, 5].

Naturally, the materials for such scaffolds must be biocompatible, biodegradable materials that can be processed to porous structures; polymeric materials offer great possibilities in design and processing, and they are can be chemically modified to match a wide range of properties of first importance in biomedical applications, like mechanical properties, diffusivity, density, hydrophilicity, etc. The material used here, polycaprolactone, is a wide-spread biocompatible and biodegradable aliphatic polyester, with low melting point and good solubility in most solvents; this material found various applications in biomedical devices as urethral catheters, drug delivery systems and resorbable sutures [6], and has been proposed as a material for tissue engineering of bone and cartilage [4–7].

There are various modes of processing scaffolds, from phase separation to particle leaching, including freeze drying of a mix, polymerization in presence of a solvent, etc. The difficulty resides most of the times in controlling the internal three-dimensional architecture; indeed, scaffolds need a certain grade of porosity to allow cell seeding and proliferation, as well as interconnected pore structure to permit the migration of nutrients, growth factors and metabolism residues [3–6]. On that account, the technique to be used must provide some reproducibility and control

M. Lebourg (✉) · R. Sabater Serra · J. Más Estellés ·
J. L. Gómez Ribelles · J. Suay Antón
Center for Biomaterials, Universidad Politécnica de Valencia,
Camino de Vera s/n, Valencia 46022, Spain
e-mail: myle1@doctor.upv.es

F. Hernández Sánchez
Centro de Investigación Científica del Yucatán, C.43 No 130
Chuburná de Hidalgo, Mérida CP 97200, Mexico

J. L. Gómez Ribelles
Centro de Investigación Príncipe Felipe, Ciudad de las Artes y
las Ciencias, Valencia 46000, Spain

on the morphology. One of the pore architecture of interest is that consisting of spherical interconnected pores in which the pore size and the diameter of the pore throats can be controlled [8–11]. In the work described in this paper, a porogen technique was used to synthesize scaffolds with varying porosity and pore interconnectivity. A template was obtained by sintering spherical porogen particles in a method similar to the one used by Ma and Choi [7] to produce polylactide scaffolds and by some of us to produce acrylic scaffolds [11]. The synthesized scaffolds were characterized in terms of morphology by SEM observation and mechanically with compression tests. Future studies on this material will include the influence of the porosity on cell seeding and proliferation.

2 Materials and methods

2.1 Materials

PCL with molecular weight $10,000 \div 20,000$ Da. was purchased from Polysciences and was used without further purification. Microspheres of Elvacite 2043 (a mixture of low weight poly(ethyl methacrylate) and poly(methyl methacrylate)) were purchased from Lucite International. Ethanol, 98 % pure, was obtained from Scharlab.

2.2 Preparation of the scaffolds

2.2.1 Template preparation

Acrylic resin microspheres were used as a porogen. The template was prepared by sintering the particles in a mould constituted of two glass plates in a press. This mould filled with acrylic microspheres was heated at $140\text{ }^{\circ}\text{C}$ for 30 min to obtain the first template. This template shows the highest porosity attainable in the template (that will yield the lowest porosity of the scaffold) with classical compaction values of 60–65% for random compacted monosized spherical particles. For further compression, to obtain scaffolds with higher porosity, the thickness of the obtained disc was first measured; then the disc was replaced in the mould and compressed at $140\text{ }^{\circ}\text{C}$ for half an hour. The degree of compression was quantified by measuring the thickness loss. A series of templates with varying degrees of compression were prepared.

2.2.2 Injection of the polycaprolactone

Polycaprolactone melt was injected in the template in the device presented in Fig. 1. The template disc was placed on

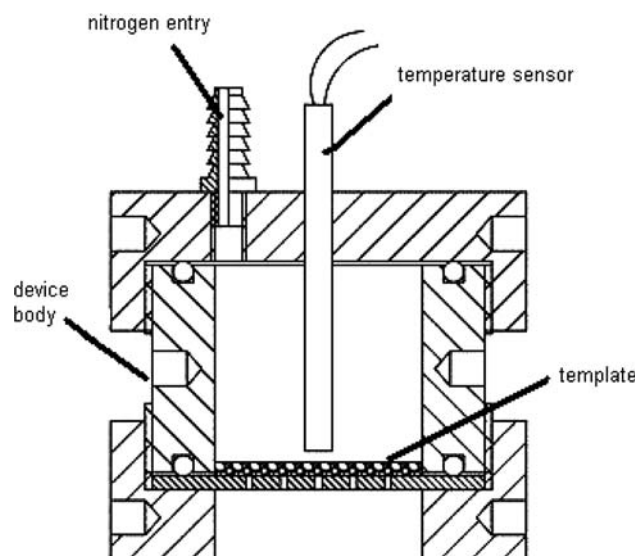


Fig. 1 Schema of the device used to introduce melted polycaprolactone in the template

the bottom of the device covered with approximately 2 g of PCL beads. The upper piece was screwed on, and connected to the nitrogen entry; then device was heated during 30 min at $110\text{ }^{\circ}\text{C}$ to melt the PCL. Then, the nitrogen pressure was set on at 5 bars until the melt began to flow out of the bores. Then the pressure was put off, the device was removed from the oven, dismantled and the disc was cooled after eliminating the excess of PCL melt on the upper side.

2.2.3 Elimination of the porogen

After cooling, the discs were immersed in ethanol, at room temperature, in order to dissolve the porogen. The solvent was changed every day until no more PEMA was detected in the solution. Then the scaffold was removed from ethanol and dried in vacuum for at least two days. Prior to measurements the scaffolds were stored in a vessel with desiccant particles.

2.3 Porosity measurements

The porosity was measured using gravimetric methods. The samples were weighed dry, and then filled with distilled water under vacuum, and subsequently weighed again. Porosity was calculated as the quotient of the volume of pores (see below) and the total volume of the scaffold.

The volume of pores, V_{pore} , was deduced from the weight difference between dry (m_{dry}) and wet (m_{wet})

sample, according to equation (1) assuming that the amount of water absorbed by the PCL phase is negligible due to its high hydrophobicity [12]. Thus, the volume of pores equals the volume occupied by the absorbed water.

$$V_{\text{pore}} = \frac{m_{\text{wet}} - m_{\text{dry}}}{d_{\text{water}}} \quad (1)$$

where d_{water} is the density of water.

The volume of polycaprolactone was calculated from the dry weight of the scaffold assuming a density of PCL about 1.135 g cm^{-3} , which corresponds to the average crystallinity measured by DSC about 63.6%. Density was calculated on the basis of amorphous phase and crystalline phase densities of respectively 1.021 and 1.2 g cm^{-3} [13].

For each sample type, at least five measurements were carried out and the obtained values were averaged.

2.4 Morphological observation with SEM

Scaffold morphologies were examined with a JEOL JSM 6300 scanning electron microscope in secondary mode. Samples were mounted on copper stubs and gold coated using a sputter coater. The microscope was used with a working distance of 18 mm and an acceleration tension of 10 kV. Manual analysis of the images was carried out in order to obtain quantitative information on scaffold morphology. For each image at least 20 pore throats were measured, taking the longer diameter in the cases where the throat appeared elliptical because of perspective.

2.5 Mechanical testing

Mechanical testing was performed using a Microtest universal testing machine with 15 N load cell, except for bulk sample where a 500 N load cell was used. Cylindrical samples of 2 mm diameter and around 2 mm height were cut with circular stamps and surgical scalpels, and then they were compressed at a rate of 0.06 mm min^{-1} until a force of 14 N was reached. Elastic modulus of the scaffold was determined using a stress strain representation. Methodology for curve interpretation and modulus calculation was taken from ASTM D1621-04a standard “Compressive properties of rigid cellular plastics”. The results presented are average values of at least five measurements.

2.6 Differential scanning calorimetry

Samples were analysed in a Perkin Elmer Pyris 1 calorimeter in heating scans from room temperature to $80 \text{ }^{\circ}\text{C}$. Crystallinity was determined by fusion enthalpy method,

with the value $\Delta H_{100\% \text{crystal}} = 139.5 \text{ J g}^{-1}$ [14]. Measurements were performed on samples after compression measurements to verify if permanent strain after compression was associated with an increase in crystallinity.

3 Results and discussion

Homogenous templates were obtained by sintering the polymeric particles of porogen. The temperature was set over the glass transition temperature of the porogen to promote neck formation between microspheres. Temperatures around 60 degrees above T_g allow good control of the sintering process without excessive deformation of the porogen. In this way the pores maintain the spherical shape of the porogen microspheres. A small pressure was applied at room temperature before heating so that the compaction was homogenous, and the limited thickness of the template avoided an inhomogenous repartition of the constraints during sintering as may occur with thicker samples.

Scaffolds with good interconnected structure and physical integrity were synthesized successfully. The semi-crystalline character of polycaprolactone prevents the structure from collapsing during or after drying: so the pore structures remain open and apt for cell spreading and fluid diffusion throughout it [4, 5].

Porosities from 60% to 85% were reached, with mean pore dimensions of 200 microns. Typical values of porosity for scaffolds studied to date are approximately 70–90% [4–7]. The porosity was seen to be related to the degree of compression during the sintering process of the template in a non linear way. Figure 2 shows results obtained relating the obtained porosity with the compressive strain applied to the template. The increase of the porosity of the scaffold finally obtained with an increase of the compression strain of the template is smaller at high compression levels. There is some scattering in the results that can be due to the memory effect of the porogen particles: when the

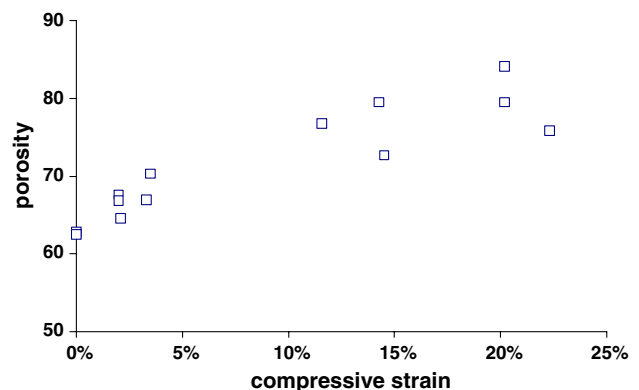
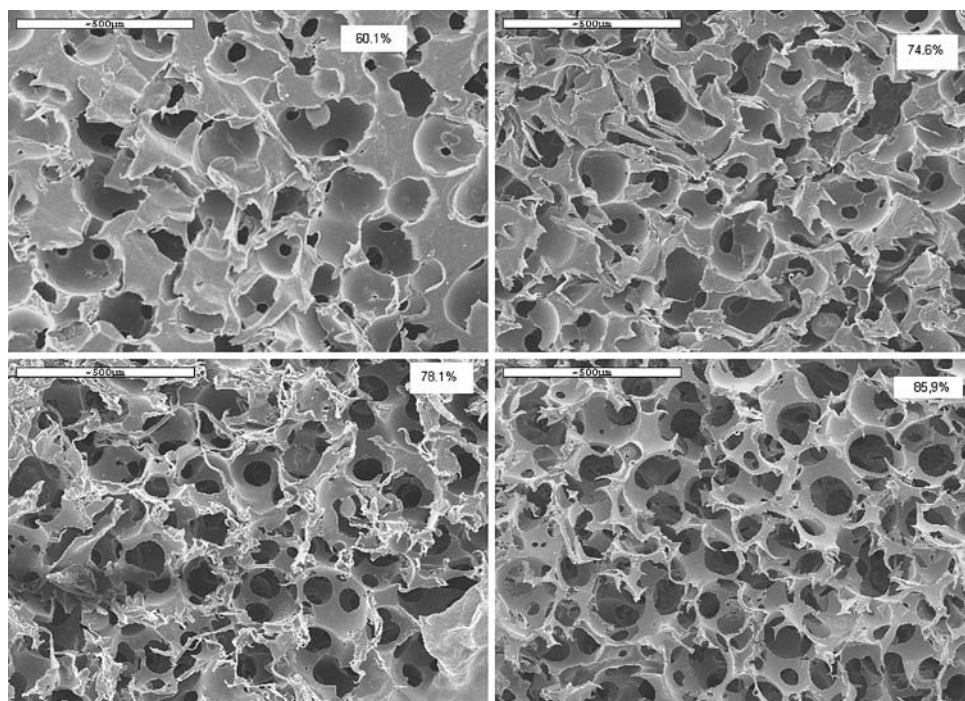


Fig. 2 Relation of porosity with the compression grade of the templates

Fig. 3 SEM microphotographs of scaffolds of different porosity (shown on each picture)



temperature of the template reaches 120 °C during PCL injection a part of the deformation suffered by the material during sintering process can be recovered and this process is poorly reproducible. This fact impedes a precise control of the porosity of the scaffold. With this technique it appeared impossible to reach a porosity higher than 85% in the scaffolds because the viscosity of the melt does not permit injection in more compact templates: the melt cannot pass through the template and it results in only a superficial injection.

The observation with electron microscopy reveals a quite homogenous structure, and well interconnected spherical pores (Fig. 3). No traces of remaining porogen can be seen. The structure is naturally more porous when the compression degree in the sintering of the template increases; particularly the pore throats are much larger for higher compaction levels. This has been said to have a significant influence on the properties of biocompatibility and cell proliferation. A systematic pore throat measurement gave the results reported on Table 1.

As expected, when the porogen microspheres are sintered only by a thermal treatment (a scaffold with a porosity of 60.1%), most of the spherical pores obtained in the scaffold are connected to the rest of the neighbour pores by very small throats, with diameters under 40 microns.

Nevertheless, nearly no isolated pores were observed. In the other extreme highly porous scaffolds shows a fully interconnected porous structure in which each spherical cavity is connected to between four and six neighbour pores through throats whose diameter reaches 80 microns, nearly a half of the average pore diameter.

Well interconnected structures, as those shown by these scaffolds, are indispensable in tissue engineering issues, they allow the migration of cells into the scaffold, and permit the good diffusion of nutriment and eventually signalling substances throughout the structure, which represents a basic condition for tissue regeneration [4, 5]. Pore throat size is related with the permeability and diffusivity throughout the material, and thus with the survival of implanted cells. The most porous structures are more likely to offer good conditions for cell spreading, because of their greater specific surface area. However, they are more likely to crumble under wear conditions, which could be a serious drawback in vivo, because of crumb release in the environment, which is known to set up acute inflammation reaction [4, 5].

Then, it is worth noting that the average diameter of the pores coincides with that of the porogen particles, i.e., during porogen extraction in ethanol, although some of the solvent can be absorbed by the PCL matrix (hot ethanol is a solvent for PCL) the effect of swelling of the PCL matrix

Table 1 Mean diameter of the pore connection throats

Porosity	60.1 ± 0.7	74.6 ± 1.6	78.1 ± 0.5	85.9 ± 2.4
Mean diameter of the pore throats (µm)	38.3	52.7	71.9	82.3

and subsequent drying produces no significant dimensional changes in the scaffold. So the size of the pores is directly related to the diameter of the porogen microspheres used, whereas the interconnections between pores are related to the compression during sintering process.

The results of the mechanical tests were interpreted in terms of stress–strain curves. The experimental curve shown in Fig. 4 for scaffolds with varying porosities is representative of the set of results obtained. The behaviour shown agrees with the typical curves obtained in the compression of foams [15]. The first zone of the curve corresponds to surface adaptation to the testing machine, because of defects in the planarity of the samples. The ASTM D1621-04a standard gives a method to discard this first zone of “accommodation” by a tangent method, which allows calculating the true “zero point” of strain and the elastic modulus, as shown in Fig. 5. All curves were adjusted with this method prior to modulus calculation.

The elastic modulus values for scaffolds of varying porosity are listed in Table 2. They range from 0.61 MPa for the most porous sample, 85.9% porosity, to 8 MPa for the less porous sample, 60% porosity. The Table 3 presents values given in the literature for hyaline cartilage compression modulus for comparison, and as can be seen, they lie in the same order of magnitude as the modulus measured for the PCL scaffolds, confirming that they could be an interesting candidate for cartilage engineering, at least on the mechanical point of view. Indeed the modulus for the more porous specimens (75% to 85%, that are more likely to be used for implantation in vivo) range from 2.5 MPa to 0.6 MPa, so they lie in the rigidity value interval reported by Athanasiou et al. [16] for human articular cartilage: between 0.51 and 1.82 MPa. This is of importance for the good regeneration of the tissue [3–5, 15]. It permits to avoid the phenomenon of stress shielding (the cells are not submitted to any

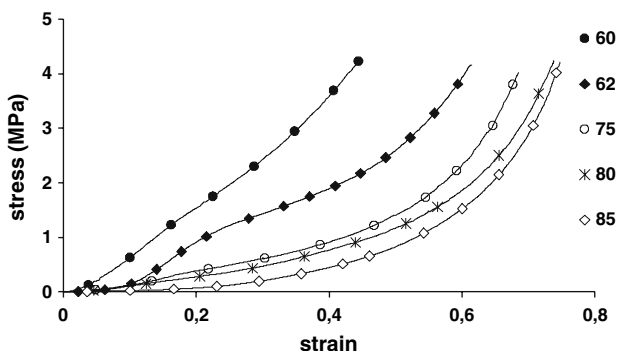


Fig. 4 Typical stress–strain compression curves measured on scaffold samples of various porosities

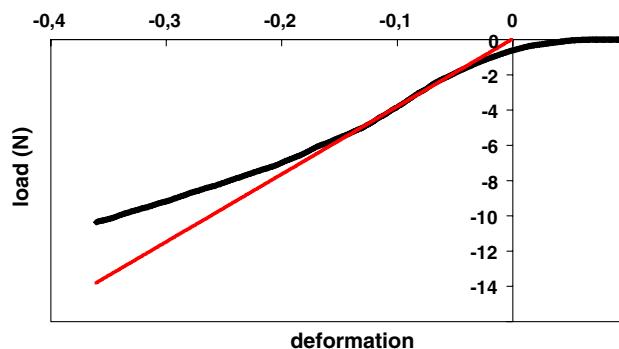


Fig. 5 Extension-load compression curve measured on a scaffold sample: example for the calculation of zero point. (sample porosity 62.6%)

tension) in the case of an implant with too high a modulus on one hand and also, to avoid on the other hand that the implanted cells be squeezed, as it could happen in a knee joint for example if the scaffold modulus was too low. An appropriate biomechanical environment has a strong influence on cell metabolism and phenotypic expression [16–19], that’s why more and more cell cultures are performed in bioreactors with implemented mechanical loading patterns [20–22]. A scaffold of polycaprolactone would provide an environment mechanically similar to the natural one and enhance the regeneration potential of the synthetic tissue.

A plot of the relative modulus (sample Young modulus E^* divided by the Young modulus of bulk polycaprolactone E_s) as a function of the squared reduced density p (density of the scaffold ρ^* divided by the bulk density ρ_s) revealed a linear dependence (Fig. 6) corresponding to the results previewed by the open cell foam mechanics theory of Ashby and Gibson [15], given by Eq. 2

$$\frac{E^*}{E_s} = C \times \left(\frac{\rho^*}{\rho_s}\right)^2 = C \times (1 - p)^2 \tag{2}$$

Despite of the scattering of the experimental results (Fig. 6), usual in porous material testing, it is worth noting that the results match remarkably well the model predictions, with a coefficient $R^2 = 0.9908$. Nevertheless, the value of the constant C calculated from our results on the PCL scaffolds is slightly lower than the prediction (0.7 instead of 1).

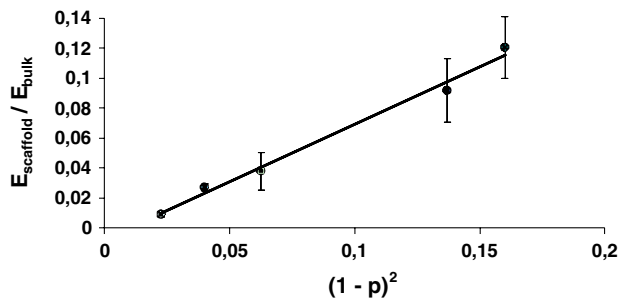
To deduce Eq. 2 Ashby and Gibson [15] considered a cell constituted by struts in a cubic lattice (see Fig. 7) where the thickness of the struts is directly related to the density of the material. In spite of the pore connectivity of our scaffolds, it seems that even for those of the highest porosity, the geometry shown in Fig. 7 is an

Table 2 Compressive modulus of PCL scaffolds

Porosity	60.1 ± 0.7	62.6 ± 2.6	74.6 ± 1.6	80.1 ± 1.6	85.9 ± 2.4
Compressive modulus E (MPa)	8.15 ± 1.38	6.2 ± 1.42	2.57 ± 0.99	1.82 ± 0.16	0.607 ± 0.12

Table 3 Literature values for mechanical properties of human cartilage

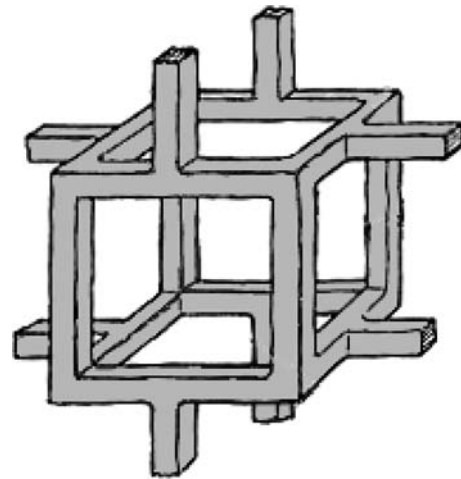
Reference	Race	Compressive modulus	Measure type	Relaxed
Athanasίου et al.	Human	0.51–1.82 MPa	Indentation/biphasic theory	No
Kempson	Human	8.4–15.3 MPa	No confined compression	Yes

**Fig. 6** Young modulus of the scaffold E^* divided by the Young modulus of bulk polycaprolactone E_s as a function of the squared reduced density p (see text)

oversimplification of the real situation. To approach more the model to the real architecture of the scaffold one could take into account that an important fraction of the material is accumulated in the cell edges while at the middle of the struts the thickness is smaller than considered in the model (see Fig. 3). This correction was studied in reference [15] in closed cell foams and yielded to the introduction of a factor, smaller than unity, affecting constant C . The same phenomenon can explain the value of constant C obtained in this work.

All scaffolds had similar crystallinity, measured by DSC, from 63.2% to 64.6 %, and this crystallinity was higher than that of the bulk sample with the same thermal history (55%) probably due to recrystallization caused by the prolonged immersion in ethanol during the porogen dissolution. After the compression test, the bulk PCL sample suffered an increase of crystallinity of 1.33%, a phase transition induced by the mechanical work applied to the sample during the experiment. Nevertheless, the scaffolds showed much smaller crystallinity change if any, probably due to the much smaller compression forces applied to them.

Further studies with cell cultures are currently conducted to determine the influence of porosity on cell proliferation rate.

**Fig. 7** Open cell model by Gibson and Ashby [15]

4 Conclusions

In this study we synthesized successfully new polycaprolactone scaffolds with interconnected spherical pores and controlled porosity, with structural porosities between 60 and 85%; no collapse of the pores was observed due to the semi-crystalline nature of polycaprolactone. The morphological study shows the interconnectivity between pores, with major pore throats when the porosity is higher. The compressive elastic modulus of samples ranges from 0.6 to 8 MPa, decreasing with increasing porosity, and lies in the value range given by literature for human articular cartilage, thus they may be able to provide a mechanically appropriate environment for cartilage engineering applications. To conclude, these scaffolds are candidates for chondrocyte culture and eventual cartilage replacement therapy.

Acknowledgements The group of the Center for Biomaterials of the UPV acknowledges the support of Spanish Ministry of Science and Education through the MAT2004-04980-C02-01 project, and the support to their research group by the Generalitat Valenciana through the project GRUPOS03/018. Julio Suay Antón acknowledges the

support of Spanish Ministry of Science and Technology through the MAT 2003-05391-C03-02 project. SEM was conducted by the authors in the Microscopy Service of the Universidad Politécnica de Valencia, whose advice is greatly appreciated.

References

1. V. BOBIC and J. NOBLE, *J. Bone Joint Surg.* **82B** (2000) 165
2. L. PETERSON, T. MINAS, M. BRITTBERG, A. NILSSON, E. SJÖGREN-JANSSON and A. LINDAHL, *Clin. Orthop.* **374** (2000) 212
3. E. B. HUNZIKER, *Osteoarthr. Carti.* **10** (2001) 432
4. C. W. Patrick Jr, A. G. Mikos and L. V. McIntire (Editors), in “Frontiers in Tissue Engineering” (Pergamon Press, Oxford 1998)
5. R. P. Lanza, R. Langer and J. Vacanti (Editors), in “Principles of Tissue Engineering” (Academic Press, San Diego, 2000)
6. A. J. Domb, J. Kost and D. M. Wiseman (Editors), in “Handbook of Biodegradable Polymers” (Harwood Academic Publishers, Amsterdam, 1997)
7. D. W. HUTMACHER, *Biomaterials* **21** (2000) 2529
8. P. X. MA and J. W. CHOI, *Tissue Eng.* **7** (2001) 23
9. V. J. CHEN and P. X. MA, *Biomaterials* **25** (2004) 2065
10. Z. MA, C. GAO, Y. GONG and J. SHEN, *J. Biomed. Mater. Res. B: Appl. Biomater.* **67B** (2003) 610
11. R. BRÍGIDO DIEGO, M. PÉREZ OLMEDILLA, A. SERRANO AROCA, J. L. GÓMEZ RIBELLES, M. MONLEÓN PRADAS, G. GALLEGO FERRER and M. SALMERÓN SÁNCHEZ, *J. Mater. Sci. Mater Med.* **16** (2005) 693
12. D. S. JONES, D. W. J. MCLAUGHLIN, C. P. MCCOY and S. P. GORMAN, *Biomaterials* **26** (2005) 1761
13. T. HAYASHI, K. NAKAYAMA, M. MOCHIZUKI and T. MASUDA, *Pure Appl. Chem.* **74** (2002) 869
14. V. CRESCENZI, G. MANZINI, G. CALZOLARI and C. BORRI, *Eur. Polym. J.* **8** (1972) 449
15. L. J. Gibson and M. F. Ashby, in “Cellular Solids-Structure and Properties” (University Press, Cambridge 1999)
16. A. J. SAMARZA and A. Athanasiou, *Ann. Biomed. Eng.* **32**(2004) 2
17. U. HANSEN, M. SCHÜNKE, C. DOMM, N. IOANNIDIS, J. HASSENPFUG, T. GEHRKE and B. KURZ, *J. Biomech.* **34** (2001) 941
18. E. M. DARLING and K. A. ANASTASIOU, *Annals Biomed. Eng.* **31** (2003) 1114
19. O. DEMARTEAU, D. WENDT, A. BRACCINI, M. JAKOB, D. SCHAFER, M. HEBERER and I. MARTIN, *Biomed. Biophys. Res. Commun.* **310** (2003) 580
20. J. S. TEMENOFF and A. G. MIKOS, *Biomaterials* **21** (2000) 431–440
21. D. J. GRIFFON, M. REZA SEDIGHI, D. V. SCHAEFFER, J. A. EURELL and A. L. JOHNSON, *Acta Biomaterialia* **2** (2006) 313–320
22. R. L. MAUCK, S. L. SEYHAN, G. A. ATESHIAN and C. T. HUNG, *Ann. Biomed. Eng.* **30** (2002) 1046–1056